International Journal of Biochemistry and Cell Biology 112 (2019) 50–60

Contents lists available at ScienceDirect

International Journal of Biochemistry and Cell Biology

journal homepage: www.elsevier.com/locate/biocel

Taurine protects against arsenic trioxide-induced insulin resistance via ROS-Autophagy pathway in skeletal muscle

Lei Yang[a,1], Tianming Qiu[a,1], Xiaofeng Yao[a], Liping Jiang[b], Sen Wei[a], Pei Pei[a], Zhidong Wang[a], Jie Bai[c], Xiaofang Liu[c], Guang Yang[c], Shuang Liu[a], Xiance Sun[a,d,*]

[a] Department of Occupational and Environment Health, Dalian Medical University, 9 W Lvshun South Road, Dalian, 116044, PR China
[b] Experimental Teaching Center of Public Health, Dalian Medical University, 9 W Lvshun South Road, Dalian, 116044, PR China
[c] Department of Nutrition & Food safety, Dalian Medical University, 9 W Lvshun South Road, Dalian, 116044, PR China
[d] Global Health Research Center, Dalian Medical University, 9 W Lvshun South Road, Dalian, 116044, PR China

ARTICLE INFO

Keywords:
Arsenic
Skeletal muscle
Insulin resistance
Autophagy
Taurine

ABSTRACT

Long-term and low-dose exposure to inorganic arsenic is associated with type 2 diabetes (T2D). In this study, C57BL/6 mice exposed to As_2O_3 showed impaired glucose tolerance, decrease in insulin sensitivity and insulin resistance were observed in the skeletal muscle and myotubes of mice that underwent As_2O_3 treatment. Decreased insulin-stimulated glucose uptake (ISGU) was also shown by the As_2O_3-treated myotubes. Moreover, the accumulation of ectopic fat in mice skeletal muscle and myotubes was observed after As_2O_3 treatment. The upregulated expression of autophagy-associated proteins and the increased number of acidic vesicular organelles (AVOs) indicated that autophagy was stimulated in the skeletal muscle and myotubes of mice after undergoing As_2O_3 treatment. TAU could prevent the effect of As_2O_3 on mice skeletal muscle and myotubes, as mentioned above. The impaired ISGU, decreased insulin-associated proteins expression, and increased TAG content caused by As_2O_3 were reversed by N-acetylcysteine (NAC) and 3-methyladenine (3-MA), and the As_2O_3-induced autophagy was inhibited by NAC, indicating involvement of ROS-autophagy pathway in the mechanism of As_2O_3-induced IR and lipid metabolism disorder. In summary, TAU protect against the As_2O_3-induced IR and ectopic fat accumulation in mice skeletal muscle and myotubes via ROS-autophagy pathway.

1. Introduction

Arsenic is a carcinogenic nonmetallic compound that is widely found in, for instance, water, coal, and air (Abbas et al., 2018). Long-term exposure to inorganic arsenic can cause cancer and skin damage, but cardiovascular disease and type 2 diabetes (T2D), which are a serious threat to human life, can develop as a consequence (Quansah et al., 2015; Webb et al., 2017). Studies have shown that exposure to low-dose As_2O_3 in drinking water is associated with an increased incidence of diabetes and that it plays an extremely important role in the pathogenesis and development of diabetes (Maull et al., 2012). Insulin resistance (IR) is formed in the early stages of diabetes and is the basis of T2D (Samuel and Shulman, 2016). Moreover, in vitro and in vivo studies have shown that there is an association between IR and arsenic levels in human tissue (Choi et al., 2014; Park et al., 2016).

Liver, skeletal muscle and adipose tissue are the three major peripheral organs that are sensitive to insulin and will show a decrease in insulin sensitivity when IR occurs (Czech, 2017). Skeletal muscle is the largest organ in the body and accounts for 45% of body composition, and it plays a major role in glucose disposal, which is responsible for consuming nearly 80% of insulin-stimulated glucose uptake (ISGU) (Periasamy et al., 2017). Insulin stimulation can promote phosphorylation of protein kinase B (Akt/PKB) and eventually promote the transfer of glucose transporter 4 (GLUT4) to the cell membrane in skeletal muscle cells (Shang et al., 2017). GLUT4 is a protein that helps the transportation of glucose into skeletal muscle cells. When IR occurs, skeletal muscle will show a significant decrease in ISGU and an impaired sensitivity to insulin (Deshmukh, 2016). Skeletal muscle with IR

Abbreviations: TAU, taurine; IR, insulin resistance; 3-MA, 3-methyladenine; NAC, N-acetylcysteine; T2D, type 2 diabetes; GLUT4, glucose transporter 4; IRS, insulin receptor substrate; ISGU, insulin-stimulated glucose uptake; HOMA-IR, Homeostasis model assessment of insulin resistance; AVOs, acidic vesicular organelles; LC3, light chain 3; CD36, fatty acid translocase; TAG, triglyceride

* Corresponding author.
E-mail address: sunxiance@dmu.edu.cn (X. Sun).

[1] The two authors contributed equally to this work.

https://doi.org/10.1016/j.biocel.2019.05.001
Received 8 January 2019; Received in revised form 9 April 2019; Accepted 2 May 2019
Available online 03 May 2019
1357-2725/

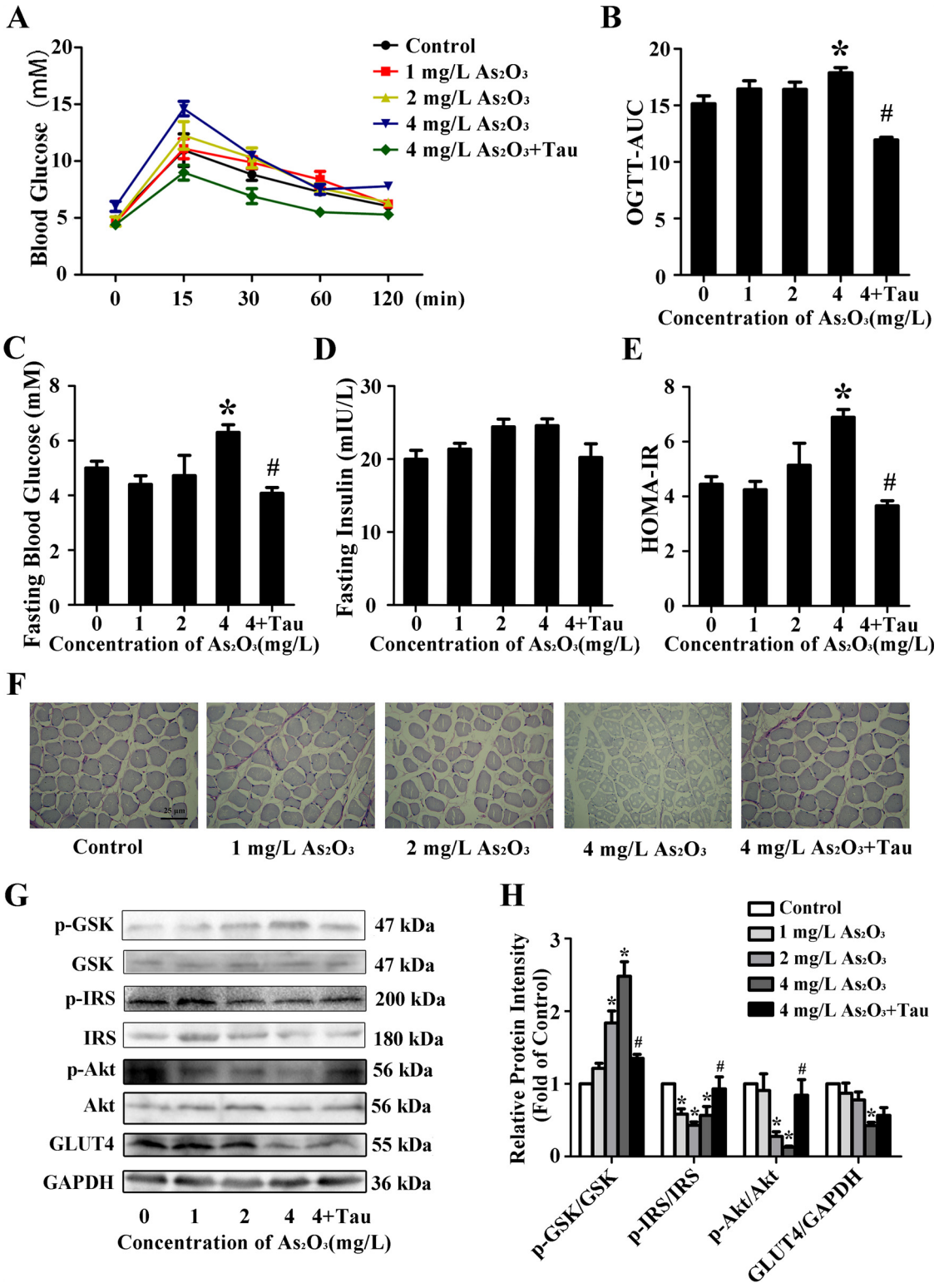

Fig. 1. TAU supplementation relieved impaired glucose tolerance in C57BL/6 mice and IR caused by As_2O_3 in mouse skeletal muscle. (A) Male C57/BL6J mice were treated with 1–4 mg/L As_2O_3 for 12 weeks. The glucose tolerance of As_2O_3-treated C57BL/6 mice was measured by OGTT. (B) OGTT-AUC in each group. (C) FBG of mice exposed to As_2O_3 was detected. (D) FINS of mice exposed to As_2O_3 was detected. (E) HOMA-IR of mice exposed to As_2O_3 was detected. HOMA-IR = FBG*FINS/22.5. (F) PAS staining of mice skeletal muscle exposed to As_2O_3 was detected. (G) The whole protein fraction was analysed by Western blot analysis. GAPDH was used as an internal control. (H) The relative expression of proteins expressed in mice skeletal muscle as described in G (n = 5). The bar represents the mean ± SEM; *P < 0.05 vs. control, #P < 0.05 vs. 4 mg/L As_2O_3 group.

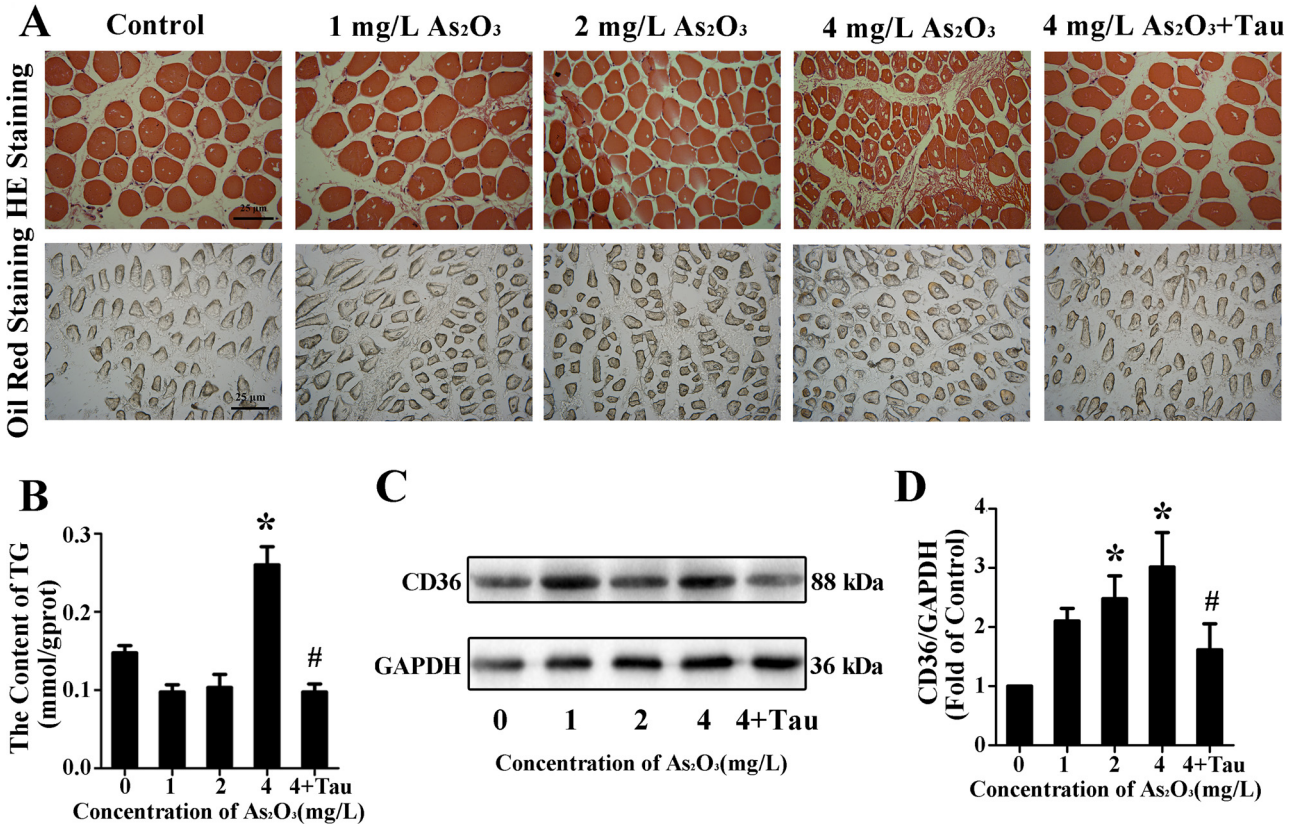

Fig. 2. As_2O_3 caused ectopic lipid accumulation in mouse skeletal muscle. (A) Male C57/BL6J mice were treated with 1–4 mg/L As_2O_3 for 12 weeks. HE staining and oil red staining of the skeletal muscle of As_2O_3-treated mice were performed. (B) The content of TAG in mice skeletal muscle exposed to As_2O_3 was measured. (C) The whole protein fraction was analysed by Western blotting. GAPDH was used as an internal control. (D) Densitometric analyses of CD36 expressed in mice skeletal muscle as described in C. The relative expression of CD36 was expressed as a percentage of the level of GAPDH (n = 5). The bar represents the mean ± SEM; *P < 0.05 vs. control, #P < 0.05 vs. 4 mg/L As_2O_3 group (For interpretation of the references to colour in this figure legend, the reader is referred to the web version of this article).

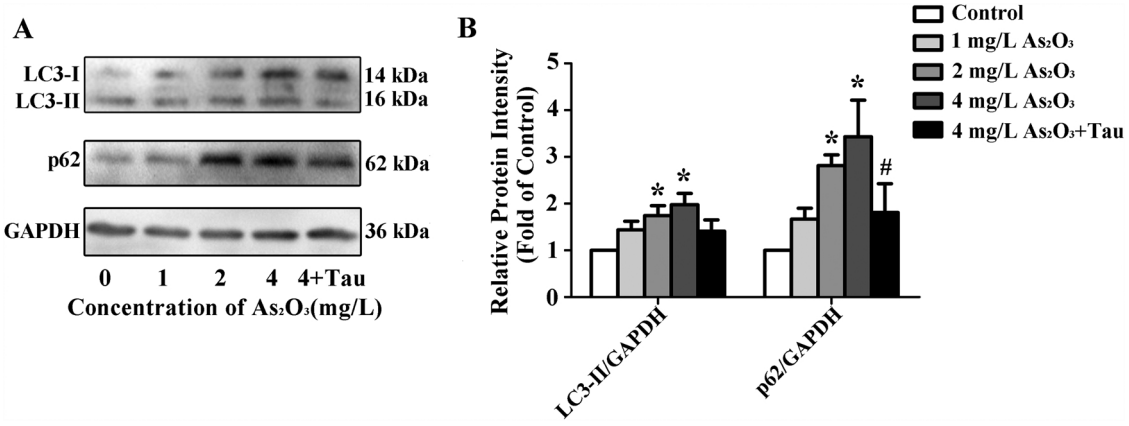

Fig. 3. TAU protected autophagy induced by As_2O_3 exposure in mouse skeletal muscle. (A) Male C57/BL6J mice were treated with 1–4 mg/L As_2O_3 for 12 weeks. The whole protein fraction was analysed by Western blotting. GAPDH was used as an internal control. (B) The relative expression of proteins expressed in mice skeletal muscle as described in A (n = 5). The bar represents the mean ± SEM; *P < 0.05 vs. control, #P < 0.05 vs. 4 mg/L As_2O_3 group.

will show not only impaired glucose metabolism but also impaired lipid metabolism. Fatty acid translocase (CD36) is a key protein in the mediation of transmembrane transportation of fatty acids. Studies have shown that expression of CD36 in peripheral organs with IR is increased significantly, leading to ectopic fat deposition (Titov, 2016). Studies have shown that T2D occurs when islets fail to secrete enough insulin to compensate for the effects of insulin resistance (Reaven, 2005). Our previous study showed that exposure to As_2O_3 causes a decrease in glucose-stimulated insulin secretion (GSIS) in islets (Wu et al., 2017). However, whether exposure to As_2O_3 can lead to IR in skeletal muscle remains unclear.

Autophagy is an intracellular recycling system that degrades cytosolic proteins and malfunctioning organelles, which is important for starvation adaptation and cellular quality control (Yoshii and Mizushima, 2017). A normal level of autophagy can help maintain cell homeostasis. However, long-term sustained stimulation can cause cellular dysfunction. Autophagy is mediated by a series of autophagy-related proteins that lead to the conversion of microtubule-associated

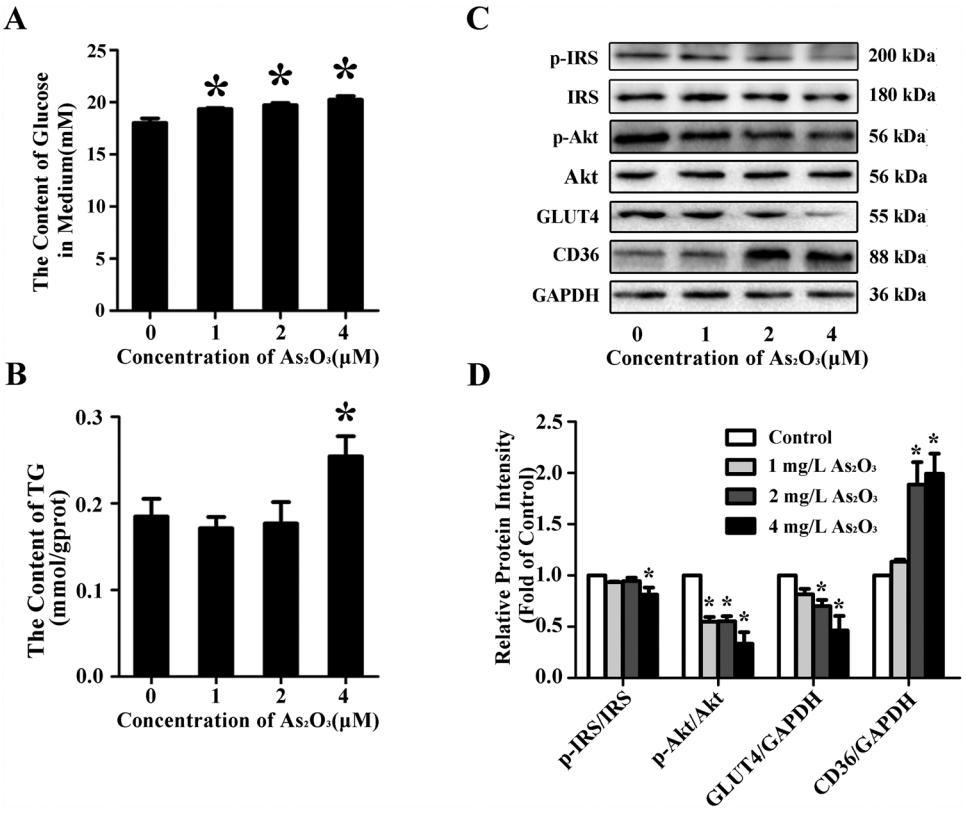

Fig. 4. As_2O_3 treatment of myotubes caused IR and ectopic fat deposition. (A) Myotubes were treated with 1–4 μM As_2O_3 for 48 h. The content of glucose in the medium of myotubes exposed to As_2O_3 was detected. (B) The content of TAG in myotubes exposed to As_2O_3 was measured. (C) The whole protein fraction was analysed by Western blotting. GAPDH was used as an internal control. (D) The relative expression of proteins expressed in mice skeletal muscle as described in C (n = 3). The bar represents the means ± SEM; *P < 0.05 vs. control.

protein 1 light chain 3 (LC3) from LC3-I to LC3-II. The expression of LC3-II represents an increase in the number of autophagolysosomes (Chen et al., 2017; Qi et al., 2014). Sequestosome 1 (p62/SQSTM1) is also a well-recognized marker associated with autophagy, and it is specifically degraded in the process of autophagy (Pankiv et al., 2007). Recent studies have reported that autophagy is involved in the pathogenesis of T2D (Sarparanta et al., 2017). Previous studies have shown that exposure to As_2O_3 can induce autophagy in islets and the liver (Bai et al., 2016b; Zhu et al., 2014), but it is not clear whether exposure to As_2O_3 can lead autophagy in skeletal muscle.

Taurine (TAU) is widely distributed in animal cells, and it is especially rich in marine animals. TAU has many healthy functions, including regulation of neurotransmission, antioxidation, and lowering of the cholesterol level in plasma (Kilb and Fukuda, 2017; Mezzomo et al., 2017). Studies have shown that TAU can improve β cell function, improve insulin secretion and maintain glucose homeostasis in diabetic mice and prevent the accumulation of white fat in mice (Mikami et al., 2012; Santos-Silva et al., 2015). Therefore, our study aims to investigate whether TAU can ameliorate As_2O_3-induced IR in skeletal muscle by inhibiting autophagy, and it provides basic data for the prevention and treatment of As_2O_3-induced T2D.

2. Materials and methods

2.1. Animals

35 male-C57BL/6 mice were obtained from the Model Animal Research Centre of Dalian Medical University (Dalian, China). The mice were housed and handled according to protocols approved by the Dalian Medical University Animal Care and Use Committee. The mice were randomly divided into 5 groups, each composed of 7 animals. As_2O_3 (CAS no. 1327-53-3) was obtained from Sigma-Aldrich. The mice were exposed to 1–4 mg/L As_2O_3 via the drinking water for 12 consecutive weeks, and those in the 4 mg/L As_2O_3 group received 250 mg/kg/d TAU via gavage.

2.2. Cell culture and treatment

In this study, an immortalised murine myoblast cell line (C2C12) was used (National Infrastructure of Cell Line Resourse, Beijing, China). Cells were cultured and maintained in DMEM media (HyClone, Thermo Scientific) supplemented with 10% foetal bovine serum (HyClone, Thermo Scientific) and a 1% mixture of penicillin and streptomycin (HyClone, Thermo Scientific), and they were incubated in 5% CO_2 at 37 °C. For differentiation of the cells into myotubes, DMEM media supplemented with 2% horse serum (HyClone, Thermo Scientific) and a 1% mixture of penicillin and streptomycin were added when the cells reached a confluence of 90%. The entire differentiation process lasted 7 days.

2.3. Oral glucose tolerance test (OGTT)

During the 12th week, OGTT was performed on the mice following 16 h of fasting. Glucose (2 g/kg body weight) was orally administered to each animal. Tail vein blood samples were obtained at 0, 15, 30, 60, and 120 min after glucose administration.

2.4. Haematoxylin-eosin (HE) staining

The parts of the mice skeletal muscles that underwent As_2O_3 treatment were isolated and fixed in saturated picric acid solution. After 48 h, they were washed in 70% alcohol until there was no picric solution precipitation. Then, the skeletal muscle were treated with dehydration and embedded in paraffin wax. They were then cut into 4–5 μm thick sections, which were stained with haematoxylin-eosin and subjected to pathological analysis using microscopy.

2.5. Oil red O staining

The parts of the mouse skeletal muscles that underwent As_2O_3 treatment were isolated and fixed in 10% formalin. After the specimens

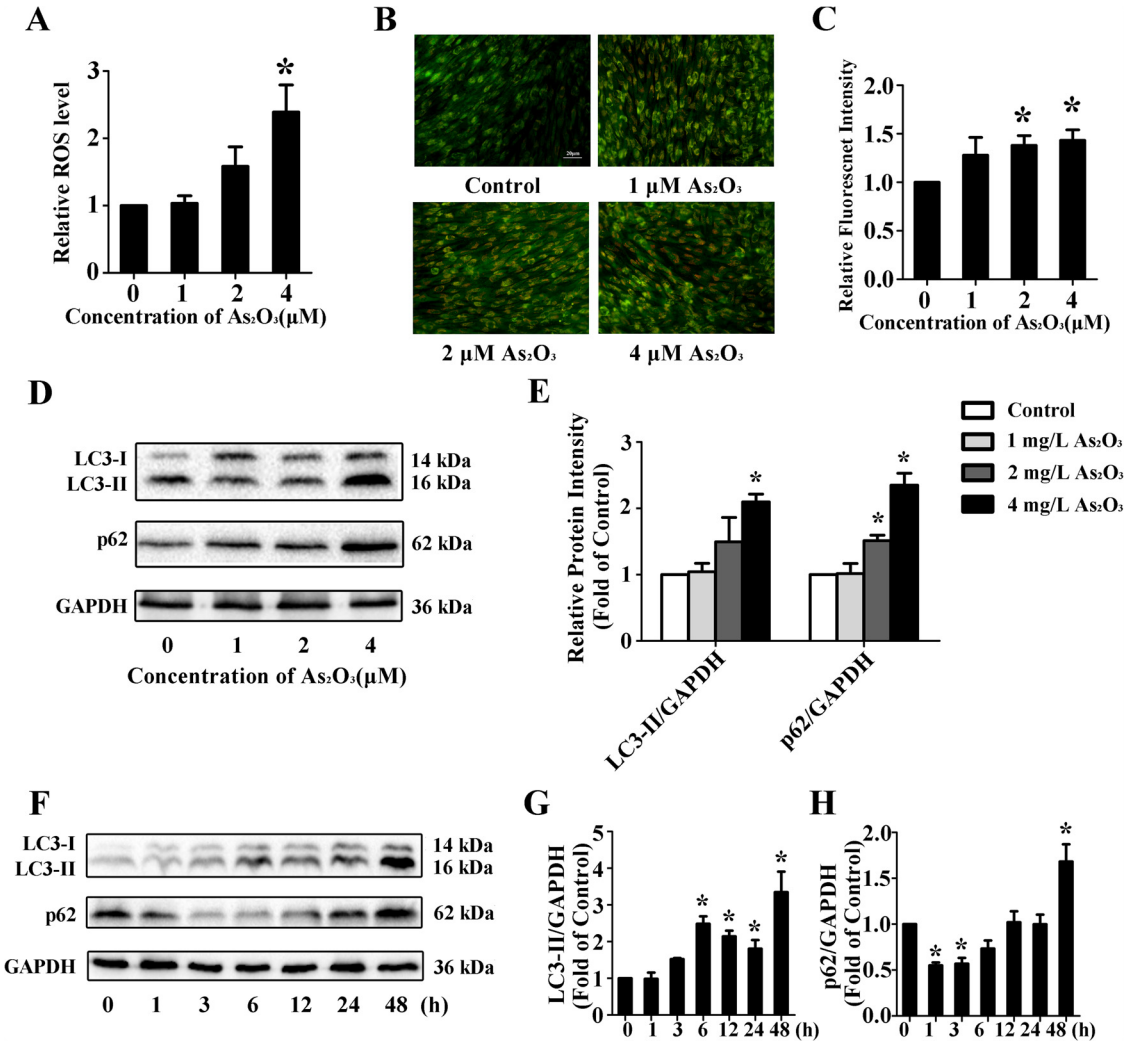

Fig. 5. Exposure to As_2O_3 induced autophagy in myotubes. (A) The quantification of ROS in myotubes (n = 3). (B) Formation of autophagolysosomes in myotubes was measured by AO staining. (C) Quantitation of formation of autophagolysosomes in As_2O_3-treated myotubes was performed (n = 3). (D) Myotubes were treated with 1–4 μM As_2O_3 for 48 h. The whole protein fraction was analysed by Western blotting. GAPDH was used as an internal control. (E) The relative expression of proteins expressed in mice skeletal muscle as described in D (n = 3). (F) Myotubes were treated with 4 μM As_2O_3 for 1–48 h. The whole protein fraction was analysed by Western blotting. GAPDH was used as an internal control. (G) Densitometric analyses of LC3-II expressed in myotubes as described in G. The relative expression of LC3-II was expressed as a percentage of the level of GAPDH (n = 3). (H) Densitometric analyses of p62 expressed in myotubes as described in G (n = 3). The bar represents the mean ± SEM; *P < 0.05 vs. control.

were dehydrated in a graded sucrose solution series, sections of tissue (thickness of 10 μm) were prepared and stained with oil red O (Wanleibio) at 60 °C for 10 min. After differentiation in 75% ethanol for 1.5 min. the staining distribution was visualized by microscopy.

2.6. Periodic acid-Schiff (PAS) staining

The skeletal muscle sections of mice treated with As_2O_3 were dewaxed in xylene and hydrated in alcohol. Then, the sections were oxidated with periodic acid solution and combined with colourless magenta in Schiff's solution. After they were counterstained with haematoxylin, the sections were closured with neutral resin and subjected to pathological analysis using microscopy.

2.7. Western blot analysis

The skeletal muscle samples of mice treated with As_2O_3 stored at −80 °C were homogenized. The supernatant was collected using RIPA lysis buffer, and the supernatant of myotubes treated with As_2O_3 was collected using a nuclear protein and cytoplasmic protein extraction kit (KGP1100). The total protein content was measured using the BCA method (Thermo Scientific). Lysates were resolved by 10–15% SDS-PAGE and transferred to a PVDF membrane. They were immunoblotted with primary antibodies against LC3B (Abcam), p62 (Proteintech), p-Akt (Abcam), Akt (Proteintech), GLUT4 (Wanleibio), GSK3β (Wanleibio), p-GSK3β (Wanleibio), IRS^{-1} (Cell Signaling Technology), p-IRS^{-1} (ABclonal), CD36 (Wanleibio), and GAPDH (Proteintech). The blots were then incubated with horseradish peroxidase (HRP)-conjugated secondary antibodies (Sigma), followed by undergoing detection with a SuperSignal West Pico kit (Thermo Scientific). The expected protein bands were visualized using the Bio-Rad ChemiDoc™ MP imaging system.

2.8. Acridine orange (AO) staining

Acridine orange (AO) (Invitrogen) was used to measure the number of acidic vesicular organelles (AVOs), such as autophagolysosomes, in cells. In intact lysosomes and autophagolysosomes, AO (AHO^+) exhibits bright red fluorescence. In contrast, the fluorescence is green. After undergoing treatment with As_2O_3, the myotubes were incubated

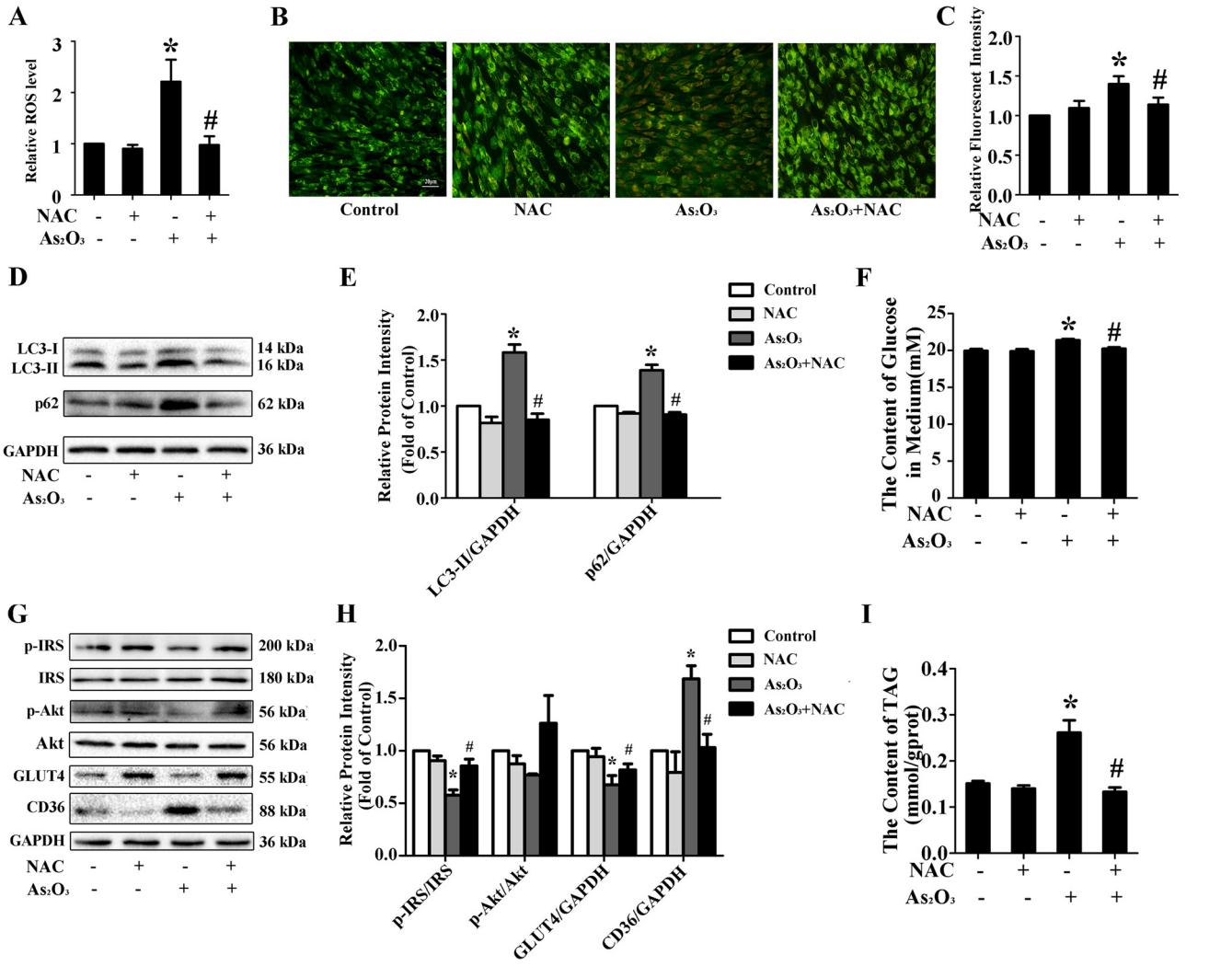

Fig. 6. Inhibition of oxidative stress protected from As_2O_3-induced IR in myotubes. (A) Quantitation of ROS in As_2O_3-treated myotubes (n = 3). (B) Formation of autophagolysosomes in myotubes was measured by AO staining. (C) Quantitation of formation of autophagolysosomes in As_2O_3-treated myotubes was performed (n = 3). (D) The whole protein fraction was analysed by Western blot. GAPDH was used as an internal control. (E) The relative expression of proteins expressed in mice skeletal muscle as described in D. (n = 3). (F) The content of glucose in medium of myotubes was measured. (G) The whole protein fraction was analysed by Western blot. GAPDH was used as an internal control. (H) The relative expression of proteins expressed in mice skeletal muscle as described in I (n = 3). (I) The content of TAG in myotubes was detected. *P < 0.05 vs. control, #P < 0.05 vs. 4 μM As_2O_3 group.

with AO (1 μg/mL) for 15 min at 37 °C and observed by fluorescence microscopy.

2.9. Measurement of intracellular reactive oxygen species

The reagent 2,7-dichlorodihydrofluorescein diacetate (DCFH-DA) was used to determine the total cell ROS level. After undergoing treatment with As_2O_3, the myotubes were washed in Ringer solution, stained with DCFH-DA at a final concentration of 10 μM at 37 °C for 30 min in the dark and observed by fluorescence microscopy.

2.10. TAG assay

The As_2O_3-treated mouse skeletal muscle samples stored at -80 °C were homogenized. The myotubes that underwent As_2O_3 treatment were frozen and melted repeatedly for a total of 3 times. The supernatant of mice skeletal muscle and myotubes treated with As_2O_3 were collected using PBS buffer. The total TAG content was measured by a triglyceride (TAG) assay kit (GPO-PAP method) (Nanjing Jiancheng Bioengineering Institute).

2.11. ISGU assay

Cells were seeded into a 96-well culture plate. After the cells underwent treatment with As_2O_3, 50 μL differentiation media with 100 nM insulin were added into each well for 2 h. Next, the media were collected. The content of glucose in the media was measured by a glucose (Glu) assay kit (Nanjing Jiancheng Bioengineering Institute).

2.12. Statistical analysis

The data were expressed as the mean ± SEM from at least three independent experiments and were analysed using SPSS 20.0 statistical software (IBM). The statistical analysis was carried out with one-way ANOVA followed by Student-Newman Keuls (SNK) test, and P < 0.05 was considered to be statistically significant.

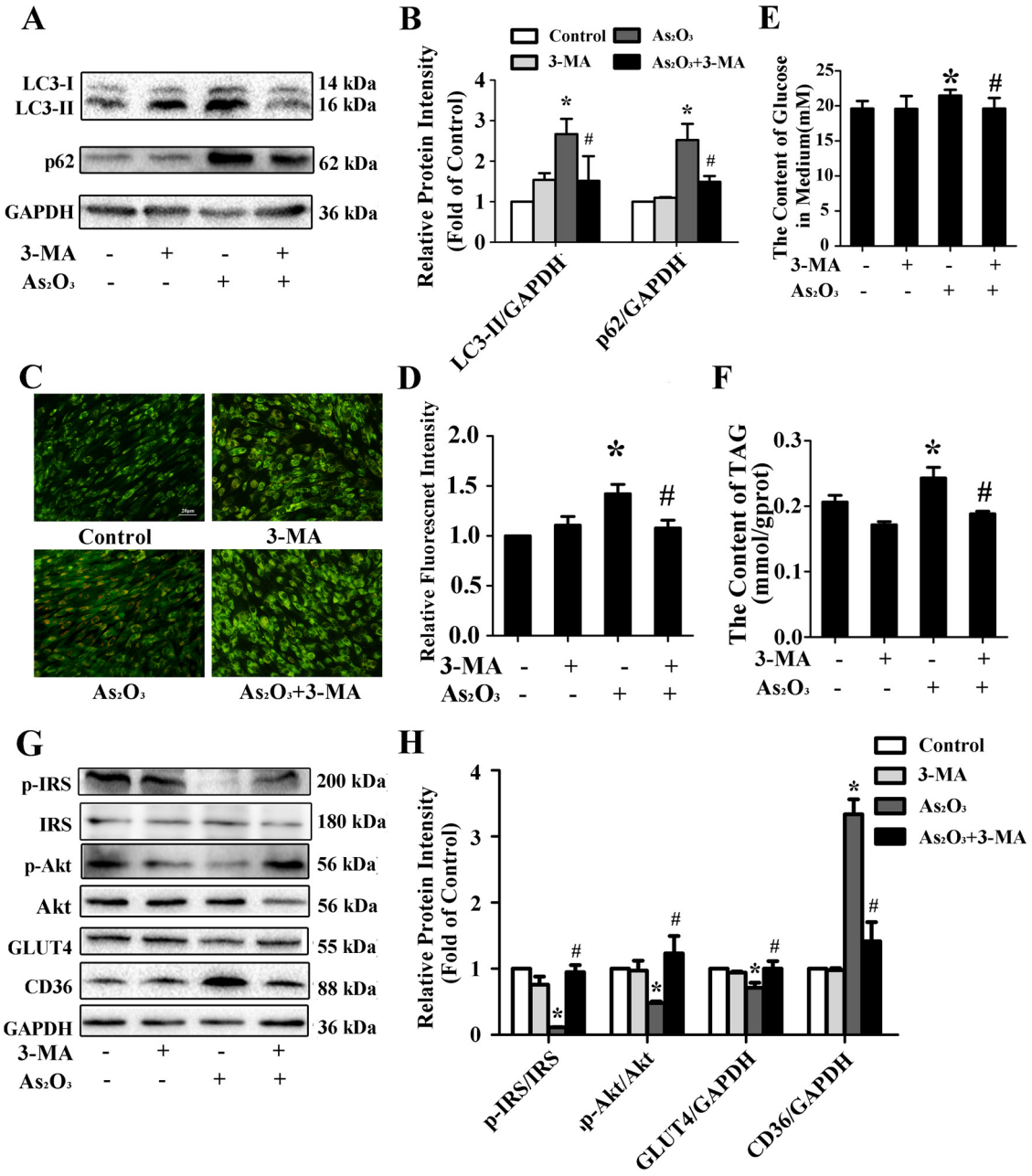

Fig. 7. Effect of autophagy on As_2O_3-induced IR in myotubes. (A) Myotubes were pretreated with 5 mM 3-MA for 3 h, and differentiation medium containing 4 μM As_2O_3 was then added consecutively for 48 h. The whole protein fraction was analysed by Western blot. GAPDH was used as an internal control. (B) The relative expression of proteins expressed in mice skeletal muscle as described in A (n = 3). (C) Formation of autophagolysosomes in myotubes was measured by AO staining. (D) Quantitation of the formation of autophagolysosomes was performed (n = 3). (E) The content of glucose in the medium of myotubes was detected. (F) The content of TAG in myotubes was measured. (G) The whole protein fraction was analysed by Western blot. GAPDH was used as an internal control. (H) The relative expression of proteins expressed in mice skeletal muscle as described in G. (n = 3). The bar represents the mean ± SEM; *P < 0.05 vs. control, #P < 0.05 vs. 4 μM As_2O_3 group.

3. Results

3.1. As_2O_3-impaired glucose tolerance in C57BL/6 mice and insulin sensitivity in mouse skeletal muscle were alleviated by TAU

The results of the OGTT showed that at 0, 15, 30, and 120 min, the average blood glucose of mice with 4 mg/L As_2O_3 treatment was significantly higher than that of mice in the control group. Additionally, the average blood glucose of mice pretreated with TAU was lower than that of mice with 4 mg/L As_2O_3 treatment (Fig. 1A). The results of the OGTT area under the curve (OGTT-AUC) showed that the average OGTT-AUC of mice with 4 mg/L As_2O_3 treatment was significantly higher than that of mice in the control group and that the average OGTT-AUC of mice pretreated with TAU was lower than that of mice with 4 mg/L As_2O_3 treatment, indicating that mice with As_2O_3 treatment showed an impaired glucose tolerance, which can be alleviated by TAU (Fig. 1B). To assess the effects of As_2O_3 on glucose homeostasis, Fasting insulin (FINS) levels, Fasting Blood Glucose (FBG) and Homeostasis model assessment of insulin resistance (HOMA-IR, an indicator of systemic insulin resistance) were evaluated. FINS showed no significant difference between the groups of mice (Fig. 1D). FBG and HOMA-IR of mice with 4 mg/L As_2O_3 treatment were significantly higher than those of mice in the control group. Additionally, FBG and HOMA-IR of mice pretreated with TAU were lower than those of mice

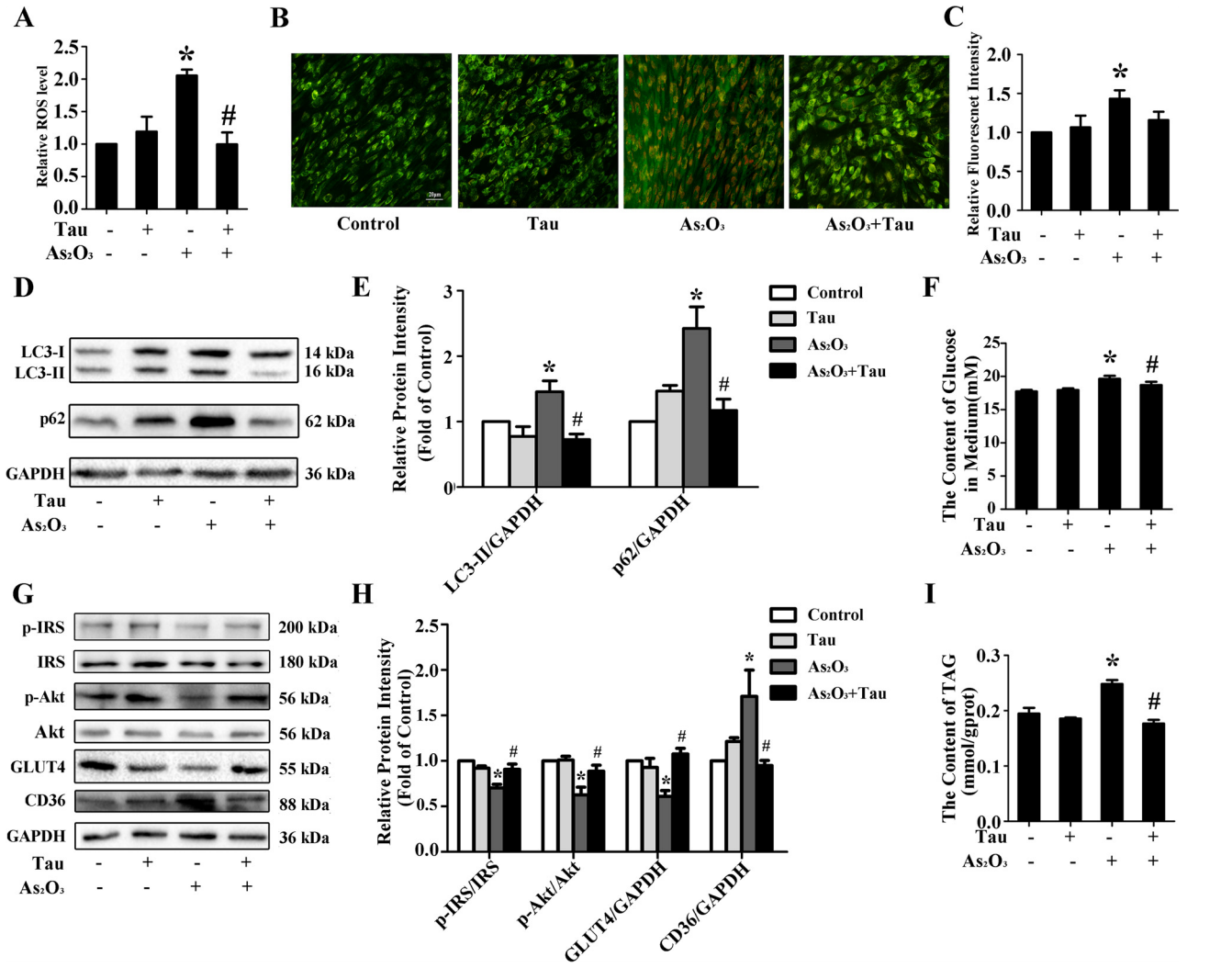

Fig. 8. TAU protected from As_2O_3-induced IR through inhibiting ROS-dependent autophagy in myotubes. Myotubes were pretreated with 100 μM TAU for 6 h, and then, differentiation medium containing 4 μM As_2O_3 was consecutively added for 48 h. (A) Quantitation of ROS in As_2O_3-treated myotubes (n = 3). (B) Formation of autophagolysosomes in myotubes was measured by AO staining. (C) Quantitation of the formation of autophagolysosomes in As_2O_3-treated myotubes was performed (n = 3). (D) The autophagy-related proteins were analysed by Western blot. GAPDH was used as an internal control. (E) The relative expression of proteins expressed in mice skeletal muscle as described in D (n = 3). (F) The content of glucose in the medium of myotubes was measured. (G) The whole protein fraction was analysed by Western blot. GAPDH was used as an internal control. (H) The relative expression of proteins expressed in mice skeletal muscle as described in I (n = 3). (I) The content of TAG in myotubes was detected. *P < 0.05 vs. control, #P < 0.05 vs. 4 μM As_2O_3 group.

with 4 mg/L As_2O_3 treatment, indicating that mice with As_2O_3 treatment showed insulin resistance, which can be alleviated by TAU (Fig. 1C, Fig. 1E). PAS staining results showed that the content of glycogen in As_2O_3-treated mice skeletal muscle was significantly decreased. However, this decrease can be relieved by TAU (Fig. 1F). Phosphorylated GSK3β was enhanced in the skeletal muscle of As_2O_3-treated mice, but this upregulation can be relieved by TAU (Fig. 1G-1 H). The ratio of p-IRS/IRS, the phosphorylation of Akt and the expression of GLUT4 in skeletal muscle of mice with As_2O_3-treated showed a significant decrease, but this decrease could be alleviated by TAU (Fig. 1G-1 H).

3.2. TAU inhibited the As_2O_3-induced ectopic fat deposition in mouse skeletal muscle

Oil red O staining showed that there was an accumulation of ectopic lipids in mouse skeletal muscles that underwent 4 mg/L As_2O_3 treatment, but this effect can be relieved by TAU (Fig. 2A). Additionally, we observed an increase in the content of TAG of mouse skeletal muscle that underwent 4 mg/L As_2O_3 treatment. However, this increase can be alleviated by TAU (Fig. 2B). The expression of CD36 in As_2O_3-treated mouse skeletal muscle was upregulated, but this upregulation can be relieved by TAU (Fig. 2C and D).

3.3. As_2O_3-upregulated autophagy in mouse skeletal muscle was relieved by TAU

To investigate whether As_2O_3 can upregulate autophagy in skeletal muscle, Western blot analysis was used to detect the expression of LC3-II and p62. The results showed that the level of LC3-II and p62 in mouse skeletal muscle with As_2O_3 treatment was upregulated, but this upregulation can be relieved by TAU (Fig. 3A-3B).

3.4. As_2O_3 induced IR in myotubes

Myotubes were exposed to different concentrations of As_2O_3 (1–4 μM) for 48 h. We measured the glucose level in the supernatant of myotubes stimulated by insulin. We observed an increase in the glucose level, suggesting that a decrease in ISGU occurred (Fig. 4A). Furthermore, the ratio of p-IRS/IRS, level of phosphorylated Akt and

expression of GLUT4 in myotubes that underwent As_2O_3 treatment gradually decreased (Fig. 4C-4D). Moreover, the content of TAG in myotubes from the 4 μM As_2O_3-treated group was higher than that in myotubes from the control group (Fig. 4B). Additionally, the level of CD36 in As_2O_3-treated myotubes increased gradually (Fig. 4C-4D).

3.5. As_2O_3 caused autophagy in myotubes

The level of the total ROS was elevated by As_2O_3 treatment (Fig. 5A). The results of AO staining showed that the number of AVOs was upregulated in the As_2O_3-treated myotubes (Fig. 5B-5C). The Western blot results showed an increase in the expression of LC3-II and p62 in the myotubes that underwent As_2O_3 treatment (Fig. 5D-5E). Then, we added differentiation medium containing 4 μM As_2O_3 for different durations (1–48 h). The results at 6 h showed an increased expression of LC3-II and a decreased level of p62 (Fig. 5F-5 H), indicating autophagy flux at an early stage of As_2O_3 treatment. However, the accumulation of p62 that was exhibited later suggests autophagy degradation disorder.

3.6. Inhibition of oxidative stress could protect from IR and ectopic fat deposition induced by As_2O_3 in myotubes

Inhibition of oxidative stress relieved ROS accumulation in As_2O_3-treated myotubes (Fig. 6A). The pretreatment with NAC not only increased the levels of LC3-II and p62 but also alleviated the rising number of AVOs in myotubes caused by As_2O_3 treatment (Fig. 6B-6E). At the same time, the content of glucose in culture medium was decreased (Fig. 6F), and the ratio of p-IRS/IRS, phosphorylation of Akt and expression of GLUT4 were increased (Fig. 6G-6 H) compared with those in As_2O_3-treated myotubes. Moreover, NAC prevented the rising TAG content and the upregulation of CD36 expression in myotubes caused by As_2O_3 treatment (Fig. 6G-6I).

3.7. Inhibition of autophagy in myotubes relieved glucose and lipid metabolism impaired by As_2O_3

To investigate whether autophagy has an effect on glucose and lipid metabolism, we used 3-MA to inhibit autophagy caused by As_2O_3. The results showed that the upregulation of LC3-II and p62 expression caused by As_2O_3 treatment was relieved (Fig. 7A-7B). The results of AO staining also showed alleviation of the high number of AVOs caused by As_2O_3 treatment (Fig. 7C-7D). With pretreatment with 3-MA, a rise in glucose level in the supernatant of myotubes caused by As_2O_3 was decreased, suggesting alleviation of ISGU (Fig. 7E). Additionally, upregulation of the phosphorylation of IRS, ratio of p-Akt/Akt and level of GLUT4 caused by As_2O_3 treatment was also relieved (Fig. 7G-7 H). Moreover, the high content of TAG and the upregulated expression of CD36 in myotubes caused by As_2O_3 treatment showed a decrease from pretreatment with 3-MA (Fig. 7F, Fig. 7G).

3.8. TAU could protect from IR and ectopic fat deposition induced by As_2O_3 through inhibiting autophagy in myotubes

The ROS accumulation in myotubes caused by As_2O_3 treatement could be relieved by TAU (Fig. 8A). With pretreatment of TAU, the rising number of AVOs in myotubes caused by As_2O_3 treatment and upregulation of LC3-II and p62 levels were alleviated (Fig. 8B-8E). At the same time, the As_2O_3-impaired glucose uptake was improved by TAU (Fig. 8F). Furthermore, the phosphorylation of IRS, ratio of p-Akt/Akt and expression of GLUT4 in the TAU-pretreated myotubes were increased (Fig. 8G-8 H) compared with those in the As_2O_3-treated myotubes. Moreover, TAU prevented the rise in TAG content and upregulation of CD36 expression in myotubes caused by As_2O_3 treatment (Fig. 8G-8I).

4. Discussion

In some studies, 25 and 50 mg/L or 20 and 40 mg/L As_2O_3 were chosen to create the chronic exposure model(Ahangarpour et al., 2018; Sun et al., 2018). However, people from most areas in the world show low-dose and long-term exposure to arsenic in drinking water(Paul et al., 2013; Phung et al., 2017). Therefore, in our study, C57BL/6 mice were exposed to 1–4 mg/L As_2O_3 in drinking water for 12 weeks, and myotubes were exposed to 1–4 μM As_2O_3 for 48 h.

Furthermore, GLUT4, one of the insulin-regulatable glucose transporter (IRGT), undergoes translocation from an intracellular site to the cell surface after exposure to insulin(Cushman and Wardzala, 1980). Therefore, the transportation of glucose can be promoted by increasing the translocation of GLUT4 to the cell membrane (Lauritzen, 2013; Ploug et al., 1998). When T2D or IR occurs, the redistribution of GLUT4 vesicles to the cell surface is reduced, resulting in a decrease in ISGU (Pinto-Junior et al., 2018; Zhang et al., 2018). However, long-term decline in the transportation of glucose is still associated with decreased expression of GLUT4(Correa-Giannella and Machado, 2013; Gutierrez-Torres et al., 2015). Our results showed that exposure to As_2O_3 caused a decrease in the expression of GLUT4 in mice skeletal muscle and myotubes, which led to impaired glucose tolerance in mice and decreased ISGU in myotubes.

CD36 mediates the transportation of fatty acids. Exposure to arsenic causes skeletal muscle inflammation, which can promote the expression of CD36 (Ahmad et al., 2012; Romic et al., 2017). It was also found that exposure to arsenic can directly affect the expression of CD36 (Supruniuk et al., 2017). We found that exposure to As_2O_3 promotes the expression of CD36 in skeletal muscle. Moreover, exposure to arsenic can decrease the expression of peroxisome proliferator-activated receptor gamma coactivator 1-α (PGC-1α), which promotes lipid oxidation in skeletal muscle (Padmaja Divya et al., 2015; Summermatter et al., 2010), resulting in an increase in the content of TAG. Our result showed an increase in the content of TAG in As_2O_3-treated mice skeletal muscle and myotubes, resulting in ectopic lipid accumulation in skeletal muscle. It has been confirmed that accumulation of ectopic lipids promotes the induction of IR (Morales and Bucarey, 2017).

Previous studies have found that arsenic accelerated autophagolysosomes formation and caused autophagic cell death in INS^{-1} and HepG2 cells (Bai et al., 2016b; Zhu et al., 2014). Controversial results have been produced regarding the effect of autophagy on IR. The activation of autophagy attenuates palmitate (PA)-induced IR in myotubes (Li et al., 2017; Wang et al., 2016). However, in the present study, autophagy exerted a stimulatory effect on IR rather than an inhibitory effect after As_2O_3 treatment. The activation of autophagy in 3T3-L1 adipocytes suppresses insulin signalling through reducing insulin-stimulated Akt phosphorylation, plasma membrane translocation of GLUT4, and glucose uptake (Zhang et al., 2016). Our results showed that exposure to As_2O_3 induces autophagy in mice skeletal muscle and myotubes. Moreover, consistent with the results from our previous study, inhibition of As_2O_3-induced ROS production alleviated autophagy, further relieving IR and ectopic fat deposition (Pan et al., 2016; Yang et al., 2018).

Consistent with the results from our previous study, TAU supplementation alleviated As_2O_3-induced autophagy (Bai et al., 2016b, 2016a). Moreover, TAU inhibits ROS production, which reduces cellular oxidative stress (Kim et al., 2017; Tappia et al., 2017). In our study, the inhibition of ROS-dependent autophagy relieved As_2O_3-induced IR and ectopic fat deposition. Based on these data, due to the availability of TAU, a variety of foods are rich in TAU, and TAU has a very good anti-insulin resistance (Gao et al., 2019) and anti-inflammatory (Qiu et al., 2018) effect, TAU can be used as a major supplement of T2D food therapy in the future.

5. Conclusions

TAU can alleviate the reduction in ISGU and ectopic lipid accumulation in mice skeletal muscle and myotubes that underwent As_2O_3 treatment by inhibiting ROS-dependent autophagy, which further alleviates IR induced by As_2O_3.

Conflicts of interest

The authors state no Conflict of interest.

Acknowledgement

This work was supported by the National Natural Science Foundation of China (NSFC, 81872566; NSFC, 81602881).

References

Abbas, G., Murtaza, B., Bibi, I., Shahid, M., Niazi, N.K., Khan, M.I., Amjad, M., Hussain, M., 2018. Arsenic uptake, toxicity, detoxification, and speciation in plants: physiological, biochemical, and molecular aspects. Int J Env. Res Public Heal. 15. https://doi.org/10.3390/ijerph15010059.

Ahangarpour, A., Zeidooni, L., Samimi, A., Alboghobeish, S., Khorsandi, L.S., Moradi, M., 2018. Chronic exposure to arsenic and high fat diet additively induced cardiotoxicity in male mice. Res. Pharm. Sci. 13, 47–56. https://doi.org/10.4103/1735-5362.220967.

Ahmad, W., Prawez, S., Chanderashekara, H.H., Tandan, S.K., Sankar, P., Sarkar, S.N., 2012. Subacute arsenic exposure through drinking water reduces the pharmacodynamic effects of ketoprofen in male rats. Env. Toxicol Pharmacol 33, 267–276. https://doi.org/10.1016/j.etap.2011.12.013.

Bai, J., Yao, X., Jiang, L., Qiu, T., Liu, S., Qi, B., Zheng, Y., Kong, Y., Yang, G., Chen, M., Liu, X., Sun, X., 2016a. Taurine protects against As2O3-induced autophagy in pancreas of rat offsprings through Nrf2/Trx pathway. Biochimie 123, 1–6. https://doi.org/10.1016/j.biochi.2016.01.002.

Bai, J., Yao, X., Jiang, L., Zhang, Q., Guan, H., Liu, S., Wu, W., Qiu, T., Gao, N., Yang, L., Yang, G., Sun, X., 2016b. Taurine protects against As2O3-induced autophagy in livers of rat offsprings through PPARγ pathway. Sci. Rep. 6, 27733. https://doi.org/10.1038/srep27733.

Chen, R., Jiang, T., She, Y., Xu, J., Li, C., Zhou, S., Shen, H., Shi, H., Liu, S., 2017. Effects of Cobalt Chloride, a Hypoxia-Mimetic Agent, on Autophagy and Atrophy in Skeletal C2C12 Myotubes. Biomed Res. Int. 2017https://doi.org/10.1155/2017/7097580. 7097580.

Choi, W.S., Kim, S.H., Chung, J.H., 2014. Relationships of hair mineral concentrations with insulin resistance in metabolic syndrome. Biol. Trace Elem. Res. 158, 323–329. https://doi.org/10.1007/s12011-014-9946-2.

Correa-Giannella, M.L., Machado, U.F., 2013. SLC2A4gene: a promising target for pharmacogenomics of insulin resistance. Pharmacogenomics 14, 847–850. https://doi.org/10.2217/pgs.13.45.

Cushman, S.W., Wardzala, L.J., 1980. Potential mechanism of insulin action on glucose transport in the isolated rat adipose cell. Apparent translocation of intracellular transport systems to the plasma membrane. J. Biol. Chem. 255, 4758–4762.

Czech, M.P., 2017. Insulin action and resistance in obesity and type 2 diabetes. Nat. Med. 23, 804–814. https://doi.org/10.1038/nm.4350.

Deshmukh, A.S., 2016. Insulin-stimulated glucose uptake in healthy and insulin-resistant skeletal muscle. Horm. Mol. Biol. Clin. Investig. 26, 13–24. https://doi.org/10.1515/hmbci-2015-0041.

Gao, N., Yao, X., Jiang, L., Yang, L., Qiu, T., Wang, Z., Pei, P., Yang, G., Liu, X., Sun, X., 2019. Taurine improves low-level inorganic arsenic-induced insulin resistance by activating PPARγ-mTORC2 signalling and inhibiting hepatic autophagy. J. Cell. Physiol. 234, 5143–5152.

Gutierrez-Torres, D.S., Gonzalez-Horta, C., Del Razo, L.M., Infante-Ramirez, R., Ramos-Martinez, E., Levario-Carrillo, M., Sanchez-Ramirez, B., 2015. Prenatal Exposure to Sodium Arsenite Alters Placental Glucose 1, 3, and 4 Transporters in Balb/c Mice. Biomed Res. Int. 2015, 175025. https://doi.org/10.1155/2015/175025.

Kilb, W., Fukuda, A., 2017. Taurine as an Essential Neuromodulator during Perinatal Cortical Development. Front. Cell. Neurosci. 11, 328. https://doi.org/10.3389/fncel.2017.00328.

Kim, Y.S., Kim, E.K., Jeon, N.J., Ryu, B.I., Hwang, J.W., Choi, E.J., Moon, S.H., Jeon, B.T., Park, P.J., 2017. Antioxidant Effect of Taurine-Rich Paroctopus dofleini Extracts Through Inhibiting ROS Production Against LPS-Induced Oxidative Stress In Vitro and In Vivo Model. Adv. Exp. Med. Biol. 975, 1165–1177. https://doi.org/10.1007/978-94-024-1079-2_93.

Lauritzen, H.P., 2013. Insulin- and contraction-induced glucose transporter 4 traffic in muscle: insights from a novel imaging approach. Exerc. Sport Sci. Rev. 41, 77–86.

Li, H., Liu, S., Yuan, H., Niu, Y., Fu, L., 2017. Sestrin 2 induces autophagy and attenuates insulin resistance by regulating AMPK signaling in C2C12 myotubes. Exp. Cell Res. 354, 18–24. https://doi.org/10.1016/j.yexcr.2017.03.023.

Maull, E.A., Ahsan, H., Edwards, J., Longnecker, M.P., Navas-Acien, A., Pi, J., Silbergeld, E.K., Styblo, M., Tseng, C.H., Thayer, K.A., Loomis, D., 2012. Evaluation of the association between arsenic and diabetes: a National Toxicology Program workshop review. Env. Heal. Perspect 120, 1658–1670. https://doi.org/10.1289/ehp.1104579.

Mezzomo, N.J., Fontana, B.D., Kalueff, A.V., Barcellos, L.J.G., Rosemberg, D.B., 2017. Understanding taurine CNS activity using alternative zebrafish models. Neurosci. Biobehav. Rev. 83, 525–539. https://doi.org/10.1016/j.neubiorev.2017.09.008.

Mikami, N., Hosokawa, M., Miyashita, K., 2012. Dietary combination of fish oil and taurine decreases fat accumulation and ameliorates blood glucose levels in type 2 diabetic/obese KK-A(y) mice. J. Food Sci. 77, H114–20. https://doi.org/10.1111/j.1750-3841.2012.02687.x.

Morales, P.E., Bucarey, J.L., 2017. Muscle Lipid Metabolism: Role of Lipid Droplets and Perilipins 2017. https://doi.org/10.1155/2017/1789395. 1789395.

Padmaja Divya, S., Pratheeshkumar, P., Son, Y.O., Vinod Roy, R., Andrew Hitron, J., Kim, D., Dai, J., Wang, L., Asha, P., Huang, B., Xu, M., Luo, J., Zhang, Z., 2015. Arsenic induces insulin resistance in mouse adipocytes and myotubes via oxidative stress-regulated mitochondrial Sirt3-FOXO3a signaling pathway. Toxicol. Sci. 146, 290–300. https://doi.org/10.1093/toxsci/kfv089.

Pan, X., Jiang, L., Zhong, L., Geng, C., Jia, L., Liu, S., Guan, H., Yang, G., Yao, X., Piao, F., Sun, X., 2016. Arsenic induces apoptosis by the lysosomal-mitochondrial pathway in INS-1 cells. Env. Toxicol 31, 133–141. https://doi.org/10.1002/tox.22027.

Pankiv, S., Clausen, T.H., Lamark, T., Brech, A., Bruun, J.A., Outzen, H., Overvatn, A., Bjorkoy, G., Johansen, T., 2007. p62/SQSTM1 binds directly to Atg8/LC3 to facilitate degradation of ubiquitinated protein aggregates by autophagy. J. Biol. Chem. 282, 24131–24145. https://doi.org/10.1074/jbc.M702824200.

Park, S.K., Peng, Q., Bielak, L.F., Silver, K.D., Peyser, P.A., Mitchell, B.D., 2016. Arsenic exposure is associated with diminished insulin sensitivity in non-diabetic Amish adults. Diabetes Metab. Res. Rev. 32, 565–571. https://doi.org/10.1002/dmrr.2769.

Paul, S., Bhattacharjee, P., Mishra, P.K., Chatterjee, D., Biswas, A., Deb, D., Ghosh, A., Mazumder, D.N., Giri, A.K., 2013. Human urothelial micronucleus assay to assess genotoxic recovery by reduction of arsenic in drinking water: a cohort study in West Bengal. India. Biometals 26, 855–862. https://doi.org/10.1007/s10534-013-9652-0.

Periasamy, M., Herrera, J.L., Reis, F.C.G., 2017. Skeletal muscle thermogenesis and its role in whole body energy metabolism. Diabetes Metab. J. 41, 327–336. https://doi.org/10.4093/dmj.2017.41.5.327.

Phung, D., Connell, D., Rutherford, S., Chu, C., 2017. Cardiovascular risk from water arsenic exposure in Vietnam: application of systematic review and meta-regression analysis in chemical health risk assessment. Chemosphere 177, 167–175. https://doi.org/10.1016/j.chemosphere.2017.03.012.

Pinto-Junior, D.C., Silva, K.S., Michalani, M.L., Yonamine, C.Y., Esteves, J.V., 2018. Advanced glycation end products-induced insulin resistance involves repression of skeletal muscle GLUT4 expression. Sci. Rep. 8, 8109. https://doi.org/10.1038/s41598-018-26482-6.

Ploug, T., Deurs Van, B., Ai, H., Cushman, S.W., Ralston, E., 1998. Analysis of GLUT4 distribution in whole skeletal muscle fibers: identification of distinct storage compartments that are recruited by insulin and muscle contractions. J. Cell Biol. 142, 1429–1446.

Qi, Y., Zhang, M., Li, H., Frank, J.A., Dai, L., Liu, H., Zhang, Z., Wang, C., Chen, G., 2014. Autophagy inhibition by sustained overproduction of IL6 contributes to arsenic carcinogenesis. Cancer Res. 74, 3740–3752. https://doi.org/10.1158/0008-5472.can-13-3182.

Qiu, T., Pei, P., Yao, X., Jiang, L., Wei, S., Wang, Z., Bai, J., Yang, G., Gao, N., Yang, L., 2018. Taurine attenuates arsenic-induced pyroptosis and nonalcoholic steatohepatitis by inhibiting the autophagic-inflammasomal pathway. Cell Death Dis. 9, 946.

Quansah, R., Armah, F.A., Essumang, D.K., Luginaah, I., Clarke, E., Marfoh, K., Cobbina, S.J., Nketiah-Amponsah, E., Namujju, P.B., Obiri, S., Dzodzomenyo, M., 2015. Association of arsenic with adverse pregnancy outcomes/infant mortality: a systematic review and meta-analysis. Env. Heal. Perspect 123, 412–421. https://doi.org/10.1289/ehp.1307894.

Reaven, G.M., 2005. The insulin resistance syndrome: definition and dietary approaches to treatment. Annu. Rev. Nutr. 25, 391–406. https://doi.org/10.1146/annurev.nutr.24.012003.132155.

Romic, S., Krskova, K., Olszanecki, R., Balazova, L., Lory, V., Koricanac, G., Slamkova, M., Zorad, S., 2017. Obesity- and age-related alterations in FAT/CD36 translocation and lipin-1 subcellular localization in skeletal muscle of the Zucker rats. Gen. Physiol. Biophys. 36, 399–406. https://doi.org/10.4149/gpb_2017010.

Samuel, V.T., Shulman, G.I., 2016. The pathogenesis of insulin resistance: integrating signaling pathways and substrate flux. J. Clin. Invest. 126, 12–22. https://doi.org/10.1172/jci77812.

Santos-Silva, J.C., Ribeiro, R.A., Vettorazzi, J.F., Irles, E., Rickli, S., Borck, P.C., Porciuncula, P.M., Quesada, I., Nadal, A., Boschero, A.C., Carneiro, E.M., 2015. Taurine supplementation ameliorates glucose homeostasis, prevents insulin and glucagon hypersecretion, and controls β, α, and δ-cell masses in genetic obese mice. Amino Acids 47, 1533–1548. https://doi.org/10.1007/s00726-015-1988-z.

Sarparanta, J., Garcia-Macia, M., Singh, R., 2017. Autophagy and mitochondria in obesity and type 2 diabetes. Curr. Diabetes Rev. 13, 352–369. https://doi.org/10.2174/1573399812666160217122530.

Shang, L., Chen, T., Deng, Y., Huang, Y., Huang, Y., Xian, J., Lu, W., Yang, L., Huang, Q., 2017. Caveolin-3 promotes glycometabolism, growth and proliferation in muscle cells. PLoS One 12, e0189004. https://doi.org/10.1371/journal.pone.0189004.

Summermatter, S., Baum, O., Santos, G., Hoppeler, H., Handschin, C., 2010. Peroxisome Proliferator-activated Receptor γ Coactivator 1α (PGC-1α) Promotes Skeletal Muscle Lipid Refueling in Vivo by Activating de Novo Lipogenesis and the Pentose Phosphate Pathway. J. Biol. Chem. 285, 32793–32800. https://doi.org/10.1074/jbc.M110.145995.

Sun, Q., Yang, Q., Xu, H., Xue, J., Chen, C., Yang, X., Gao, X., Liu, Q., 2018. miR-149 negative regulation of mafA is involved in the arsenite-induced dysfunction of insulin synthesis and secretion in pancreatic beta cells. Toxicol. Sci. https://doi.org/10.1093/toxsci/kfy150.

Supruniuk, E., Miklosz, A., Chabowski, A., 2017. The Implication of PGC-1α on Fatty Acid Transport across Plasma and Mitochondrial Membranes in the Insulin Sensitive Tissues. Front. Physiol. 8, 923. https://doi.org/10.3389/fphys.2017.00923.

Tappia, P.S., Adameova, A., Dhalla, N.S., 2017. Attenuation of diabetes-induced cardiac and subcellular defects by sulphur-containing amino acids. Curr. Med. Chem. https://doi.org/10.2174/0929867324666170705115207.

Titov, V.N., 2016. The excess of palmittic fatty acid in food as main cause of lipoidosis of insulin-dependent cells: skeletal myocytes, cardio-myocytes, periportal heaptocytes, kupffer macrophages and β-cell of pancreas. Klin. Lab. Diagn. 61, 68–77.

Wang, Y., Hu, Y., Sun, C., Zhuo, S., He, Z., Wang, H., Yan, M., Liu, J., Luan, Y., Dai, C., Yang, Y., Huang, R., Zhou, B., Zhang, F., Zhai, Q., 2016. Down-regulation of Risa improves insulin sensitivity by enhancing autophagy. FASEB J. 30, 3133–3145. https://doi.org/10.1096/fj.201500058R.

Webb, E., Moon, J., Dyrszka, L., Rodriguez, B., Cox, C., Patisaul, H., Bushkin, S., London, E., 2017. Neurodevelopmental and neurological effects of chemicals associated with unconventional oil and natural gas operations and their potential effects on infants and children. Rev Env. Heal. https://doi.org/10.1515/reveh-2017-0008.

Wu, W., Yao, X., Jiang, L., Zhang, Q., Bai, J., Qiu, T., Yang, L., Gao, N., Yang, G., Liu, X., Chen, M., Sun, X., 2017. Pancreatic islet-autonomous effect of arsenic on insulin secretion through endoplasmic reticulum stress-autophagy pathway. Food Chem. Toxicol. 111, 19–26. https://doi.org/10.1016/j.fct.2017.10.043.

Yang, G., Bai, Y., Wu, X., Sun, X., Sun, M., Liu, X., Yao, X., Zhang, C., Chu, Q., Jiang, L., Wang, S., 2018. Patulin induced ROS-dependent autophagic cell death in Human Hepatoma G2 cells. Chem. Biol. Interact. 288, 24–31. https://doi.org/10.1016/j.cbi.2018.03.018.

Yoshii, S.R., Mizushima, N., 2017. Monitoring and measuring autophagy. Int. J. Mol. Sci. 18. https://doi.org/10.3390/ijms18091865.

Zhang, D., Zhang, Y., Ye, M., Ding, Y., Tang, Z., Li, M., Zhou, Y., Wang, C., 2016. Interference with Akt signaling pathway contributes curcumin-induced adipocyte insulin resistance. Mol. Cell. Endocrinol. 429, 1–9. https://doi.org/10.1016/j.mce.2016.04.013.

Zhang, C., Jiang, Y., Liu, J., Jin, M., Qin, N., Chen, Y., Niu, W., Duan, H., 2018. AMPK/AS160 mediates tiliroside derivatives-stimulated GLUT4 translocation in muscle cells. Drug Des. Devel. Ther. 12, 1581–1587. https://doi.org/10.2147/dddt.s164441.

Zhu, X.X., Yao, X.F., Jiang, L.P., Geng, C.Y., Zhong, L.F., Yang, G., Zheng, B.L., Sun, X.C., 2014. Sodium arsenite induces ROS-dependent autophagic cell death in pancreatic beta-cells. Food Chem. Toxicol. 70, 144–150. https://doi.org/10.1016/j.fct.2014.05.006.